



HAL
open science

Impact of Mesoscale Eddies on Deep Chlorophyll Maxima

Marin Cornec, R. Laxenaire, Hervé Claustre, Sabrina Speich

► **To cite this version:**

Marin Cornec, R. Laxenaire, Hervé Claustre, Sabrina Speich. Impact of Mesoscale Eddies on Deep Chlorophyll Maxima. *Geophysical Research Letters*, 2021, 48 (15), 10.1029/2021GL093470. hal-03312063

HAL Id: hal-03312063

<https://hal.science/hal-03312063>

Submitted on 3 Aug 2021

HAL is a multi-disciplinary open access archive for the deposit and dissemination of scientific research documents, whether they are published or not. The documents may come from teaching and research institutions in France or abroad, or from public or private research centers.

L'archive ouverte pluridisciplinaire **HAL**, est destinée au dépôt et à la diffusion de documents scientifiques de niveau recherche, publiés ou non, émanant des établissements d'enseignement et de recherche français ou étrangers, des laboratoires publics ou privés.



Distributed under a Creative Commons Attribution - NonCommercial - NoDerivatives 4.0 International License

Geophysical Research Letters



RESEARCH LETTER

10.1029/2021GL093470

Impact of Mesoscale Eddies on Deep Chlorophyll Maxima

Marin Cornec¹ , Rémi Laxenaire^{2,3} , Sabrina Speich³ , and Hervé Claustre¹ 

Key Points:

- Deep Chlorophyll Maxima are key biological features of stratified environments that escape satellite ocean-color detection
- The impact of mesoscale eddies on DCM is assessed by matching a global BGC-Argo database with eddies detected from satellite altimetry
- While cyclonic eddies increase biomass maxima occurrences, anticyclonic eddies favor the presence of maxima resulting from photoacclimation

Supporting Information:

Supporting Information may be found in the online version of this article.

Correspondence to:

M. Cornec,
cornec@obs-vlfr.fr

Citation:

Cornec, M., Laxenaire, R., Speich, S., & Claustre, H. (2021). Impact of mesoscale eddies on deep chlorophyll maxima. *Geophysical Research Letters*, 48, e2021GL093470. <https://doi.org/10.1029/2021GL093470>

Received 23 MAR 2021

Accepted 29 JUN 2021

¹Laboratoire d'Océanographie de Villefranche, CNRS & Sorbonne Université, LOV, Villefranche-sur-Mer, France, ²Center for Ocean-Atmospheric Prediction Studies, Florida State University, Tallahassee, FL, USA, ³Laboratoire de Météorologie Dynamique, LMD-IPSL, UMR, Ecole Polytechnique, ENS, CNRS, Paris, France

Abstract Deep Chlorophyll Maxima (DCM) are ubiquitous features in stratified oceanic systems. Their establishment and maintenance result from hydrographical stability favoring specific environmental conditions with respect to light and nutrient availability required for phytoplankton growth. This stability can potentially be challenged by mesoscale eddies impacting the water column's vertical structure and thus the environmental parameters that condition the subsistence of DCMs. Here, data from the global BGC-Argo float network are collocated with mesoscale eddies to explore their impact on DCMs. We show that cyclonic eddies, by providing optimal light and nutrient conditions, increase the occurrence of DCMs characterized by Deep Biomass Maxima for phytoplankton. In contrast, DCMs in anticyclonic eddies seem to be driven by photoacclimation as they coincide with Deep Acclimation Maxima without biomass accumulation. These findings suggest that the two types of eddies potentially have different impacts on the role of DCMs in global primary production.

Plain Language Summary In the global ocean, phytoplankton can be found at depths where their growth is limited by their access to light from the surface and nutrient supply from below. Depending on the combination of environmental conditions, phytoplankton at depth can either accumulate in densely populated layers or deploy adaptive survival strategies such as multiplying their internal light sensors. Given their dependence on environmental variations, phytoplankton can be affected by physical disturbances that alter the vertical structure of the water column's properties. Among these are mesoscale eddies, large water structures dominated by rotation on the horizontal plane which also induce vertical physical movements. In this study, we associate data from autonomous robots that drift with ocean currents and sample physical and biological properties down to a depth of 2,000 meters, with mesoscale eddies detected by satellite. We show that on a global scale, cold mesoscale eddies promote the growth of phytoplankton at depth.

1. Introduction

Deep Chlorophyll Maxima (DCM) are ubiquitous phytoplanktonic features observed in the global ocean (Baldry et al., 2020; Cornec et al., 2021; Cullen, 2015; Mignot et al., 2014; Silsbe & Malkin, 2016), and more specifically in stratified systems (Cullen, 2015; Estrada et al., 1993). These active phytoplankton layers at depth are often indiscernible via satellite observation (Joint & Groom, 2000; Platt et al., 1988). Depending on environmental conditions, a DCM can either reflect an effective accumulation of biomass (Deep Biomass Maximum, DBM, Beckmann & Hense, 2007; Cullen, 2015; Herbrand & Voituriez, 1979), or result from an increase in the chlorophyll-*a* concentration (Chl_a) of phytoplankton cellular content in response to low light levels (Deep photoAcclimation Maximum, DAM), without any associated increase of biomass (Fennel & Boss, 2003; Letelier et al., 2004; Mignot et al., 2014; Steele, 1964). DCMs, and more particularly DBMs, are likely to contribute significantly to global primary production (Cullen, 2015; Hanson et al., 2007; Silsbe & Malkin, 2016). Their occurrence and characteristics depend on a favorable combination of light and nutrient supply over time periods long enough for the development of a stable deep phytoplankton layer (Beckmann & Hense, 2007; Cullen, 2015; Huisman et al., 2006; Klausmeier & Litchman, 2001; Letelier et al., 2004). To better understand their dynamics, it is necessary to assess the drivers affecting their environmental properties, in particular, those affecting light and nutrient availability at depth.

Small-scale ocean dynamics, such as internal waves or mesoscale eddies, may act as altering factors synced with phytoplankton responses, as they can induce vertical perturbations of the water column (McGillicuddy et al., 1998; Uz et al., 2001). Mesoscale eddies are ubiquitous structures in the global ocean (Chaigneau

© 2021. The Authors.
This is an open access article under the terms of the [Creative Commons Attribution-NonCommercial-NoDerivs License](https://creativecommons.org/licenses/by-nc-nd/4.0/), which permits use and distribution in any medium, provided the original work is properly cited, the use is non-commercial and no modifications or adaptations are made.

et al., 2009; Chelton et al., 2007, 2011), which affect phytoplankton distribution via eddy pumping along the vertical (Dufois et al., 2014; Falkowski et al., 1991; Frenger et al., 2018; Gaube et al., 2014; Mahadevan et al., 2012; McGillicuddy et al., 1998; McGillicuddy, 2016; Siegel et al., 2011). At the core of cyclonic (anti-cyclonic) eddies, eddy pumping induces a shallowing (deepening) of isopycnals, which accordingly translates into an upward (downward) displacement of the nutricline with respect to a specific light horizon. The standard hypothesis regarding this paradigm is that cyclonic eddies (C) and anticyclonic eddies (AC) respectively increase and decrease the accumulation of phytoplankton biomass (McGillicuddy, 2016). However, nuances are increasingly reported in eddy mechanisms and associated phytoplankton responses, highlighting the complexity of the phenomena in play (e.g., variations in physical fields through the eddy lifetime, contribution of lateral exchanges, eddy-wind interaction, submesoscale pumping, eddy-eddy interaction: Guidi et al., 2012; Lévy et al., 2001; McGillicuddy et al., 2007; Siegel et al., 2013; Sweeney et al., 2003). Among those modulations, variations are observed between the core sector of the eddies and their edge, the latter being subject to significant vertical motions impacting submesoscale filaments and implying interactions with the surroundings waters (Klein & Lapeyre, 2009; Siegel et al., 2008; Xiu & Chai, 2020). Moreover, the respective influences of C and AC on phytoplankton dynamics are still debated (Barone et al., 2019; Brannigan, 2016; Dufois et al., 2016; Xiu & Chai, 2020).

Observations of the impact of mesoscale eddies on DCMs remain sparse, either limited to specific locations or time periods. Additionally, such impacts often differ from those observed by satellites which capture surface layers only. A general assessment and quantification of the impact of eddies on DCM characteristics as well as on light and nutrients, their main drivers, is still missing. Yet such an assessment is particularly critical for the quasi-permanently stratified subequatorial and subtropical waters as eddies may represent the key factor regulating fluctuations of environmental drivers in these stable systems (Cullen, 2015; Letelier et al., 2000).

To help fill in this gap, our study investigates the role of eddies in modifying DCM depth and intensity by driving changes in light and nutrient fields. Our analysis of DCMs relies on BGC-Argo's global data set of vertical measurements of fluorescence of Chla (Fchl_a) and optical backscattering of particles (b_{bp}) in addition to hydrological parameters and up to four additional core BGC parameters (Chai et al., 2020; Claustre et al., 2020; Roemmich et al., 2019). Fchl_a and b_{bp} are respectively proxies of the concentrations of (Chla) (Roesler et al., 2017) and particulate organic carbon (POC) (Cetinić et al., 2012; Loisel & Morel, 1998; Stramski et al., 1999), whose combined analysis allows identification of DCMs and discrimination between DAMs and DBMs (Cornec et al., 2021). Meanwhile, to probe into eddies, we co-located the global data set of BGC-Argo profiles with the TOEddies database (Laxenaire et al., 2018) providing a global atlas of mesoscale eddies automatically detected from Absolute Dynamical Topography (ADT) obtained via multi-satellite altimetry.

This study first assesses the effect of mesoscale eddies on DCMs in the world ocean regarding the impact of the eddy cores and edges for both polarities (C and AC) on the occurrence of DAMs and DBMs. DCM seasonality is then examined in the quasi-permanently stratified systems of subtropical and subequatorial waters. Finally, the influence of eddy polarity and sectors (core vs. edge) on DCM characteristics, and on the changes in environmental drivers are described.

2. Materials and Methods

2.1. BGC Argo Database Classification and Environmental Parameters Calculation

Data from 505 BGC-Argo floats (~50,000 profiles collected from 2010 to 2020, Argo, 2020) equipped with (Chla) and b_{bp} sensors (in addition to sensors for CTD [conductivity, temperature, depth], and up to four additional BGC core parameters) were processed and qualified as described in Bellacicco et al. (2019) and Wong et al. (2020). Vertical profiles were classified as presenting a DCM or not (NO) based on the analysis of bio-optical profiles (see Supporting Information, SI: Text S1, Figure S1, and Table S1). DCM profiles were then further segregated into photoacclimation (DAM) or biomass maxima (DBM) following Cornec et al. (2021). The characterization of DCM profiles was assessed through the depth of the DCM (Z_{DCM}) as well as (Chla) and b_{bp} at the DCM depth ($[Chla]_{DCM}$ and b_{bpDCM} , proxies of DCM intensity; Hopkinson & Barbeau, 2008).

To specify the environmental context of DCMs, daily integrated Photosynthetically Available Radiation (iPAR) and nitrate concentration profiles were estimated for each BGC-Argo vertical profile. Nitrate concentration at each depth was retrieved from the dissolved oxygen profiles through the neural network-based method CANYON-B (Bittig et al., 2018; Sauzède et al., 2017, see SI: Text S2). Surface values of Photosynthetically Available Radiation (PAR) were computed with a clear-sky model (Gregg & Carder, 1990), then propagated to depth using a regional attenuation coefficient based on empirical bio-optical relations with (Chla) (Cornec et al., 2021, adapted from Morel et al., 2007). Cloud-cover coefficients were applied per month and per 10°-latitude band on the PAR profiles (Cornec et al., 2021; Lacour et al., 2017). The iPAR was then derived at each profile depth by integrating the PAR profiles over the day-length (Lacour et al., 2017). The depth of the nitracline (Z_{Nit}) was calculated as the shallowest depth at which the nitrate concentration is 1 $\mu\text{mol NO}_3$ higher than the surface concentration (Cornec et al., 2021, see SI: Text S2). The iPAR value at the nitracline depth ($i\text{PAR}_{\text{Nit}}$) gives an estimation of the potential productivity of the DCM (Cullen, 2015). Average iPAR in the Mixed Layer ($\overline{i\text{PAR}_{\text{ML}}}$) gives an estimation of light availability in the upper layer of the water column, and was calculated as the average of the iPAR values within the Mixed Layer Depth (MLD). The MLD was calculated as the depth where the potential density increased by 0.03 kg m^{-3} in relation to the surface value (de Boyer Monté gut et al., 2004).

2.2. Mesoscale Eddy Database and BGC-Argo Profiles Colocation

In the geostrophic framework, mesoscale eddies can be characterized by concentric circles of Sea Surface Height (SSH), highlighting the predominance of rotation in their dynamics. This particular property has prompted the development of algorithms for automatic eddy detection from satellite altimetry maps (e.g., Chaigneau et al., 2008, 2009; Chelton et al., 2011).

In this study, we take advantage of the global eddy atlas obtained by applying the TOEddies algorithm (Laxenaire et al., 2018) to daily $0.25^\circ \times 0.25^\circ$ AVISO ADT maps produced by Ssalto/Duacs and distributed by Copernicus-Marine Environment Services, either in delayed time (1993 to early 2019) or near-real time (early 2019 to present). This algorithm identifies, on ADT maps, local maxima (minima) as the possible center of AC (C). The features are classified as eddies if the outermost closed ADT contour containing only one possible center is characterized by a difference in ADT with the center greater than 1 mm (see Laxenaire et al. (2018) for details including validation of their method using surface drifters). This closed contour defines the outer limit of each eddy, which, in general, is affected by the external field (Laxenaire et al., 2019). The eddy's core is defined as the surface encompassed by the ADT contours with the highest mean absolute azimuthal velocity.

On the basis of the resulting database, we categorized the ocean surface, and thus flagged collocated BGC-Argo profiles, according to their position, either as regions outside eddy influence, within an eddy core (either AC or C) or within an eddy edge (defined as the area between the eddy core and its outermost contour).

To obtain a climatological view of eddy presence, we computed the percentage of time per month from 2010 to 2018 (period where the ADT data were available in delayed mode) for which each pixel of the ADT maps lay in one of the three areas (outside, core and edge of eddies) defined by the TOEddies atlas. From these data, we estimated monthly and yearly climatologies covering the period of the BGC-Argo sampling by computing mean values (respectively monthly and yearly) of the percentage of occurrence per pixel for each eddy polarity and area (i.e., AC_{core} , AC_{edge} , C_{core} and C_{edge}).

2.3. Database Regionalization and Calculation of the Anomalies of the Parameters

To assess the global distribution of DCMs and their typology (DAM or DBM), as well as the occurrence of eddies, we grouped the data of BGC-Argo profile types (SI: Table S2) per seven 20°-latitude bands centered on the Equator and up to 70° in both hemispheres (Figure 1). The BGC-Argo database's representativeness of eddy occurrence was verified by comparison with the TOEddies climatologies (SI: Text S3 and Figure S2).

For each eddy, we computed the proportions of DAM and DBM profiles, which we then compared to those outside eddy influence (i.e., EXT). We also defined the difference in percentage of DAMs and DBMs between

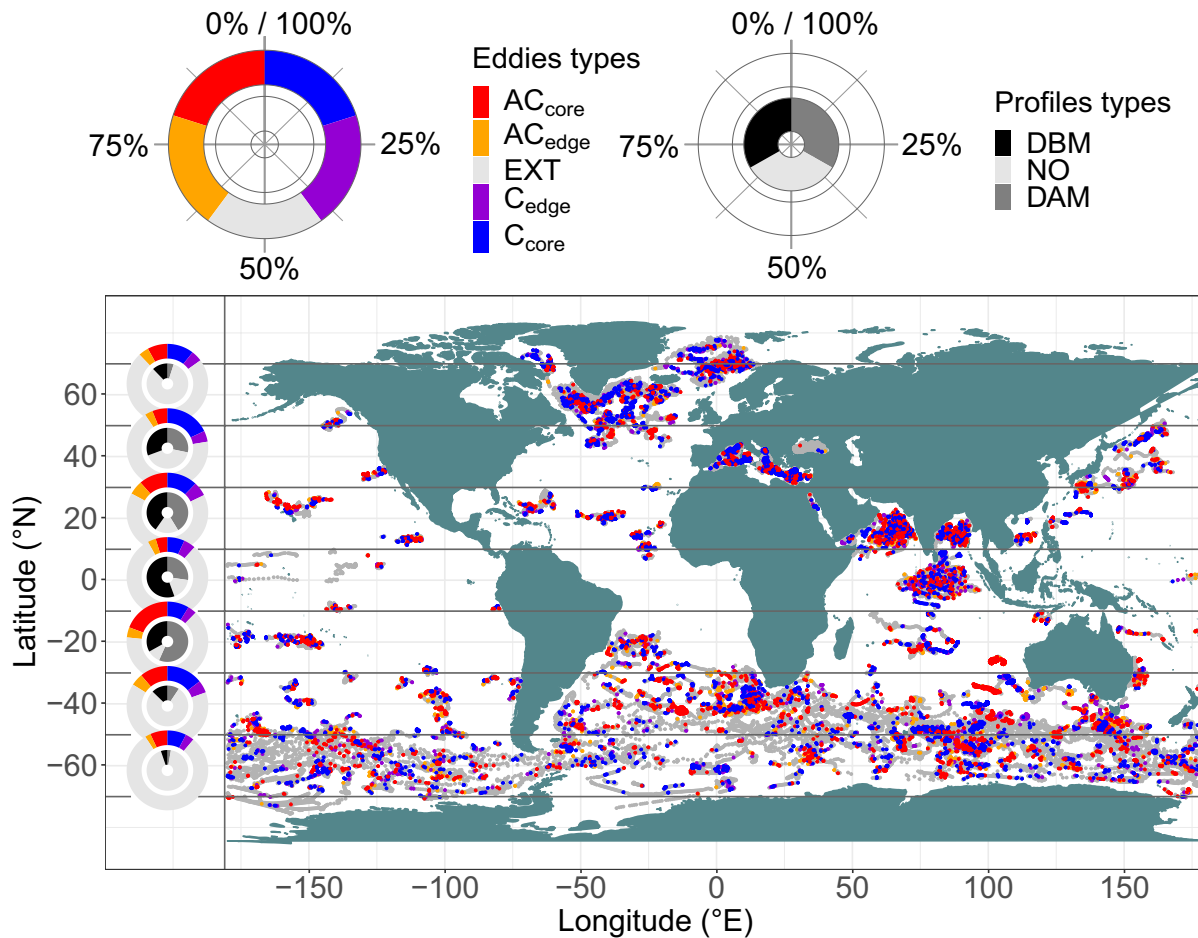


Figure 1. Map of the BGC-Argo profile database and percentages of distributions of profile types regarding to their biological types (No deep maxima, Deep photoAcclimation Maximum, and Deep Biomass Maximum; inner circles), and mean percentages of eddy polarities and sections regarding to the BGC-Argo database sampling (Cyclonic eddies and Anticyclonic eddies cores and edges, outside of eddy influence; outer circles) per 20°-latitude bands (black lines). The color of the points corresponds to the profile position regarding to eddies presence, polarity and section (same color scale as for the outer circles).

each eddy types (i.e., AC_{core} , AC_{edge} , C_{core} and C_{edge}) and with EXT as a metric of DCM anomalies associated with the presence of mesoscale eddies. We computed such anomalies on both global and monthly scales. Note that we shifted the southern hemisphere by 6 months to phase with northern-hemisphere seasonality.

We divided the subequatorial (0~15°) and subtropical latitudes (15~30°), as well as the two basins of the Mediterranean Sea which present characteristics of quasi-stratified systems, into 14 different regions with coherent a priori hydrographical and/or biogeochemical patterns to which we assigned the BGC Argo floats (Cornec et al., 2021, SI: Tables S3–S4 and Figure S3). We also computed anomalies on the same basis as described above for the three DCM descriptors ($[Chla]_{DCM}$, b_{pDCM} , and Z_{DCM}) and the four environmental parameters (Z_{Nit} , MLD, $iPAR_{Nit}$, and $iPAR_{ML}$; SI: Table S5 and Figure S4), assuming that intraregional variations of these parameters are smaller than their interregional variations.

3. Results and Discussion

3.1. Global DCM Repartition

Profiles indicating the presence of DCMs (i.e., DBM and DAM, Figure 1) dominate from 20°S to 40°N (respectively 90% and 59% of the profiles), but are less frequent at higher latitudes (respectively 17% and 8% at 60°N and 60°S). This asymmetrical distribution with comparatively higher DCM occurrence in the northern hemisphere is due to significant contribution to the data set by data from the Mediterranean Sea and Baffin

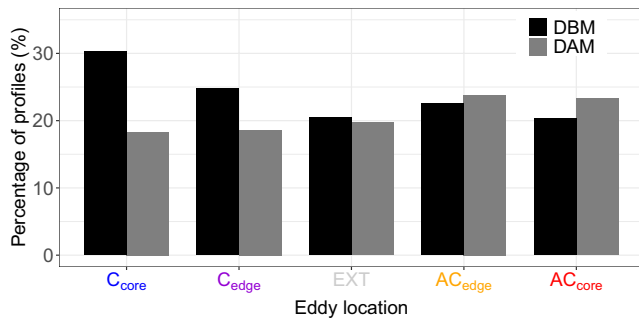


Figure 2. Percentages of Deep Biomass Maximum and Deep photoAcclimation Maxima profiles regarding to the total number of profiles within each zone (Cyclonic eddies/Anticyclonic eddies cores and edges section, and outside of eddies influence).

ing near-optimal conditions for phytoplankton to thrive at depth (Beckmann & Hense, 2007; Cullen, 2015; Herbland & Voituriez, 1979). In subtropical systems, DAM proportions increase (and dominate DCM profiles in the southern hemisphere) as deep nutriclines with low light levels lead to strong photoacclimation at the DCM depth (Letelier et al., 2004; Mignot et al., 2014).

3.2. Impact of Eddies on DAM/DBM Occurrence

Global proportions of DCM types (DAMs and DBMs) outside (EXT) and within the different eddy polarities and sections (C/AC and edge/core, Figure 2) were compared regarding the total number of profiles (including profiles with no DCMs). C present a higher occurrence of DBM profiles (30% of total profiles in C_{core}, compared to 20% in EXT), and a slightly lower proportion of DAM profiles (18% of DAM in C_{core}, compared to 20% in EXT). The opposite is true for AC: DAM occurrence increases (23%) while the DBM proportion remains steady (20%). C_{edge} present an intermediate situation between EXT and C_{core} (25% and 19% respectively for DAM and DBM profiles), whereas AC_{edge} show a higher proportion of DAM than AC_{core} (24%) and a slight increase in DBM (23%). The increased proportion of biomass accumulation profiles within C compared to those outside eddy influence suggests the former's enhancement of environmental conditions favorable to phytoplankton growth. Conversely, the environmental conditions within AC seem to favor the development of photoacclimation.

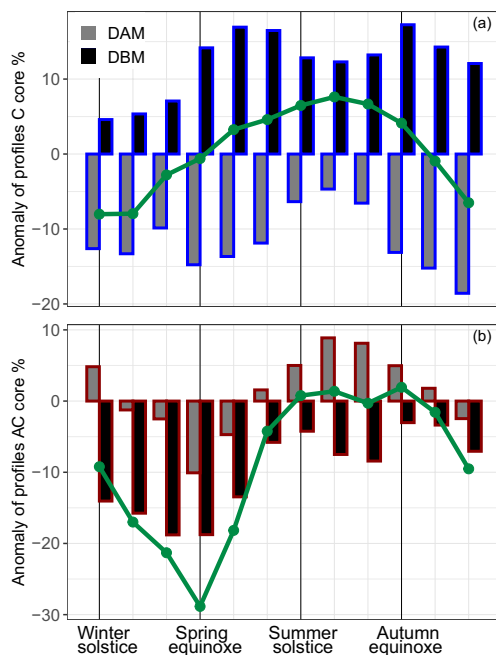


Figure 3. Monthly anomalies as percentages of each types of Deep Chlorophyll Maximum (DCM) profiles (i.e., Deep photoAcclimation Maximum or Deep Biomass Maximum) in Cyclonic eddies (a) and Anticyclonic eddies (b) cores compared to the percentages outside eddy influence within the 30°S–30°N latitudinal band. The green line represents total DCM profile anomalies. The seasonality determination is appropriate for both hemispheres, in accordance of how it is treated in the main text.

Bay, both regions presenting a strong seasonal occurrence of DCM profiles (Ardyna et al., 2011; Barbioux et al., 2019; Martin et al., 2010). DCMs are generally dominated by DBMs in the equatorial band (67% of DCM profiles at 0°), DAMs at 20°S (63%), and DBMs at 60° in both hemispheres (respectively 63% and 75% in the southern and northern hemispheres) whereas both types have equal proportions at 20°N and 40°N. The low occurrence of DCMs at high latitudes is related to their highly seasonal dynamics both in terms of hydrographical conditions and surface primary production. At those latitudes, DCMs occur during a short period (i.e., in summer) when the water column is stratified and organic material in the upper layer undergoes post-bloom depletion (Ardyna et al., 2013; Baldry et al., 2020). The high occurrence of DCMs in subequatorial and subtropical water systems confirms the quasi-permanence of upper-water stratification and organic depletion at these latitudes (Hervand & Voituriez, 1979; Letelier et al., 2004; Mignot et al., 2014). Subequatorial systems (from 0 to ~15°) are more favorable to DBM occurrence, suggest-

The issue of how seasonality affects eddy influence on DCMs was specifically addressed for the 30°S–30°N latitudinal band where DCMs are nearly permanent year-round. This sample thus excludes high-latitude regions where DCMs only develop during summer in both hemispheres. We analyzed the monthly anomalies of DBM and DAM profiles within C_{core} and AC_{core} and compared these to their occurrence outside eddy influence (Figures 3a and 3b). In C_{core}, DBM anomalies are always positive, and DAMs always negative, suggesting a system where biomass accumulation at depth dominates and photoacclimation processes are depreciated. A global increase in total DCM anomalies occurs after the spring equinox (+3%) to the autumn equinox (+4%), with a peak after the summer solstice (+8%). This period is marked by a lesser decrease in DAM proportion (−4%) and a strong increase in DBMs (+17% after the spring equinox, and at the autumn equinox). However, from late fall to early spring, the global DCM proportion decreases with a minimum around the winter solstice (−8%). Still positive but reduced, the DBM anomaly (+5%) is dominated by the strong decrease in DAM proportion. This

Bay, both regions presenting a strong seasonal occurrence of DCM profiles (Ardyna et al., 2011; Barbioux et al., 2019; Martin et al., 2010). DCMs are generally dominated by DBMs in the equatorial band (67% of DCM profiles at 0°), DAMs at 20°S (63%), and DBMs at 60° in both hemispheres (respectively 63% and 75% in the southern and northern hemispheres) whereas both types have equal proportions at 20°N and 40°N. The low occurrence of DCMs at high latitudes is related to their highly seasonal dynamics both in terms of hydrographical conditions and surface primary production. At those latitudes, DCMs occur during a short period (i.e., in summer) when the water column is stratified and organic material in the upper layer undergoes post-bloom depletion (Ardyna et al., 2013; Baldry et al., 2020). The high occurrence of DCMs in subequatorial and subtropical water systems confirms the quasi-permanence of upper-water stratification and organic depletion at these latitudes (Hervand & Voituriez, 1979; Letelier et al., 2004; Mignot et al., 2014). Subequatorial systems (from 0 to ~15°) are more favorable to DBM occurrence, suggest-

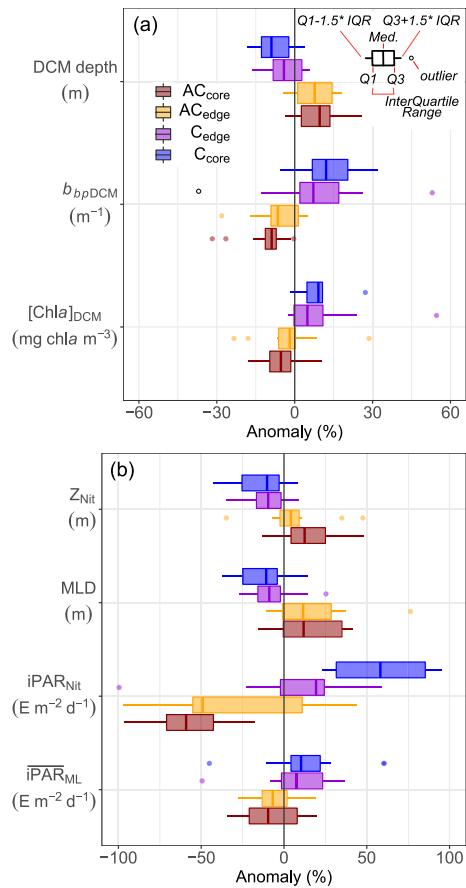


Figure 4. Quartile diagrams of regional anomalies of Deep Chlorophyll Maximum profile characteristics (a) and environmental parameters (b) for the stratified regions as a function of their location within each eddy zone (Cyclonic eddies/Anticyclonic eddies cores and edges section), all four locations being compared to the parameters outside eddy influence, that is, outside of eddies influence.

sections 3.1 and 3.2 (Figures 2 and 3). The opposite is observed in AC, with a deepening of the Z_{DCM} (+10% in AC_{core} and +8% in AC_{edge}), associated with a decrease in DCM intensity (−5% and −2% for b_{bpDCM} , −9% and −6% for $[Chla]_{DCM}$, respectively in AC_{core} and in AC_{edge}). These analyses confirm recent observations of DCM characteristics within AC and C (Barone et al., 2019; Li & Hansell, 2016; Gao et al., 2017; Pasqueron De Fommervault et al., 2017; Xiu & Chai, 2020).

As for environmental parameters, uplift of the Z_{Nit} and MLD are observed in C (Figure 4b: respectively −10% and −11% in AC_{core}, and −9% for both parameters in AC_{edge}). Positive anomalies are also recorded for $iPAR_{Nit}$ (+62% in C_{core} and +23% in C_{edge}) and $iPAR_{ML}$ (+11% in C_{core} and +7% in C_{edge}). Meanwhile, AC eddies present the reverse features: a downward shift of the Z_{Nit} (+13% in AC_{core} and +4% in AC_{edge}) and MLD (+12% in both sections), and negative anomalies for $iPAR_{Nit}$ (−60% in AC_{core} and −49% in AC_{edge}) and $iPAR_{ML}$ (−10% in AC_{core} and −7% in AC_{edge}). These estimates show that on average, C favor environmental conditions in which DCMs thrive. They suggest that the typical vertical isopycnal shoaling at their center (represented by the shallowing of the MLD in the anomalies) maintains an uplift of the nitracline (Chai et al., 2020; Vaillancourt et al., 2003). This upward shift toward the sunlit layer leads to an increase in $iPAR_{Nit}$, as observed by Letelier et al. (2000) and Hopkinson & Barbeau (2008). Meanwhile, the reverse occurs for AC: the downward displacement of isopycnals in eddy cores distances the nitracline from the euphotic zone, deterring phytoplankton growth. The fact that the edge sectors of the eddies shows an intermediate

implies that during late autumn-early winter, even if the proportion of DBMs in C_{core} increases, there is a net decrease in the total proportion of DCMs compared to the regions located outside the eddies. This decrease could result in surface blooms (as suggested by an increase in $[Chla]$ in the upper layer and a decrease in $(iPAR_{ML})$ in profiles showing no DCM compared to profiles with a DCM, SI: Figure S5) resulting from a possible injection of nutrient following an erosion of the nitracline.

In AC_{core}, total DCM anomalies are essentially negative (with a peak at the spring equinox of −29%) or close to zero in summer. These results highlight that AC disfavor the presence of DCMs. Throughout the year, DBM anomalies are also negative, with a peak before and at the spring equinox (−19%). However, DAM anomalies become positive from late spring to the autumn with a maximum after the summer solstice (+9%). The period around the summer solstice represents a critical period in the DAM/DBM transition, especially in oligotrophic systems, as this is when light penetrates deeper in the water column, hence enhancing the probability of more photons reaching the nitracline. These conditions favor biomass accumulation until the autumnal uplift of isolumes (Letelier et al., 2004; Mignot et al., 2014) when AC_{core} again tend to diminish DBMs and favor DAMs instead.

3.3. Impact of Eddies on DCM Properties and Their Environment

For stratified regions, mean anomalies of the descriptors of DCM properties (Figure 4a) and of associated environmental parameters (Figure 4b) were computed for C and AC for the 14 regions of stratified systems. For both types of descriptors, C and AC clearly present opposite effects (Mann Whitney test, p -values <0.05), with the behavior of properties within the edge sector of eddies being intermediate in relation to that in their cores (however not significantly different) or outside the eddies. In C, DCM depth shallows (Figure 4a, −9% in C_{core} and −6% in C_{edge}), combined with a significant increase of its intensity as shown by positive anomalies in b_{bpDCM} (+9% in C_{core} and +5% in C_{edge}) and $[Chla]_{DCM}$ (+12% in C_{core} and +7% in C_{edge}). The simultaneous increase in b_{bpDCM} and $[Chla]_{DCM}$ can explain the transition toward deep biomass accumulation observed in

condition may be due to the attenuation of the pumping effect by other processes (e.g., submesoscale and Ekman-induced pumping, Gaube et al., 2014; Klein & Lapeyre, 2009).

4. Conclusion

In this study, we addressed the effect of mesoscale eddies on Deep Chlorophyll Maxima (DCM) characteristics as well as the environmental context that controls their development and persistence in the global ocean. To our knowledge, this study is the first to address the impact of mesoscale eddies on those deep phytoplanktonic features at the world ocean scale, combining two complementary databases. We found that at a global scale, cyclonic eddies (C) and anticyclonic eddies (AC) have opposite effects on DCM occurrence: the largest proportion of profiles with biomass maxima (DBMs) are found inside C whereas the largest proportion of photoacclimation-related maxima (DAMs) are inside AC.

In low-latitude stratified environments dominated by quasi-permanent DCMs (i.e., subtropical and sub-equatorial regions), 20%–30% of surfaces are impacted by mesoscale eddies. C favor a global shift of the system from DAMs toward DBMs. Conversely, AC lead toward the disappearance of DCMs (with an intermediate shift from DBMs toward DAMs during the summer solstice period).

In C, the strengthening of DCMs is related to an uplift of the isopycnal and nitracline toward the sunlit layer that provides an optimal environment for phytoplankton development and growth (while the opposite occurs in AC). The increase in DCMs may result from either a proliferation of the phytoplankton community typical of DCMs outside eddy influence, or from a change in the local community (Brown et al., 2008; Jyothibabu et al., 2015; Waga et al., 2019; Waite et al., 2007). The enhancement of DCM intensity in C explains the rise in DBM occurrence. Nevertheless, the reasons for DCM decrease inside the cores of C during winter still need further investigation. This decrease could be the effect of enhanced surface productivity, or a process other than eddy pumping (e.g., submesoscale processes, eddy-wind interaction or MLD effect [Lévy et al., 2001; Mahadevan, 2016; McGillicuddy et al., 2007; Siegel et al., 2011]).

Our results highlight that in C and AC, eddy pumping appears to be the dominant process and present opposite effects on DCMs, in particular in subequatorial and subtropical latitudes where environmental conditions are more stable year-round. The effect appears to be less intense but still significant within the edge regions of the eddies compared to their core. Continued expansion of the BGC-Argo fleet will allow further investigation of these processes, for example, the impact of the eddy size and intensity, the positions of eddy cores with respect to the ocean surface (e.g., Assassi et al., 2016; Laxenaire et al., 2020), as well as processes acting at the eddy edges (Klein & Lapeyre, 2009). Furthermore, the mesoscale impact of eddies on DCM intensities suggests a potential influence on associated primary production. The potential impact of these physical features on the global carbon budget should definitely be assessed.

Data Availability Statement

All BGC-Argo data are available at <https://doi.org/10.17882/42182#75239> or at <ftp://ftp.ifremer.fr/ifremer/argo/dac/>. These data were collected and made freely available by the International Argo Program and the national programs that contribute to it. (<https://argo.ucsd.edu>, <https://www.ocean-ops.org>). The Argo Program is part of the Global Ocean Observing System. The gridded altimeter products were produced by SSALTO/DUACS and distributed by the Copernicus Marine Environment Monitoring Service. The database produced for this paper is available at the following: <https://doi.org/10.17882/76733>. The authors wish to thank the Argo Data Management team (ADMT) and the BGC-Argo Data Management team (BGC ADMT).

References

- Ardyna, M., Babin, M., Gosselin, M., Devred, E., Bélanger, S., Matsuoka, A., & Tremblay, J. É. (2013). Parameterization of vertical chlorophyll a in the Arctic Ocean: Impact of the subsurface chlorophyll maximum on regional, seasonal and annual primary production estimates. *Biogeosciences*, 10(1), 1345–1399. <https://doi.org/10.5194/bgd-10-1345-2013>
- Ardyna, M., Gosselin, M., Michel, C., Poulin, M., & Tremblay, J. É. (2011). Environmental forcing of phytoplankton community structure and function in the Canadian High arctic: Contrasting oligotrophic and eutrophic regions. *Marine Ecology Progress Series*, 442, 37–57. <https://doi.org/10.3354/meps09378>

Acknowledgments

This study is a contribution to the following projects: remOcean (European Research Council, Grant agreement 246777); REFINE (European Research Council, Grant agreement 834177); SOCLIM (BNP Foundation); AtlantOS (European Union's Horizon 2020 research and innovation program, Grant 2014-633211); NAOS (Agence Nationale de la Recherche, grant agreement J11R107-F); BGC-Argo-France (CNES-TOSCA).

- Argo (2020). Argo float data and metadata from Global Data Assembly Center (Argo GDAC) – Snapshot of Argo GDAC of July 10st 2020. *SEANOE*. <https://doi.org/10.17882/42182#75239>
- Assassi, C., Morel, Y., Vandermeersch, F., Chaigneau, A., Pegliasco, C., Morrow, R., et al. (2016). An index to distinguish surface- and subsurface-intensified vortices from surface observations. *Journal of Physical Oceanography*, 46(8), 2529–2552. <https://doi.org/10.1175/JPO-D-15-0122.1>
- Baldry, K., Strutton, P. G., Hill, N. A., & Boyd, P. W. (2020). Subsurface chlorophyll-a maxima in the Southern Ocean. In *Frontiers in Marine Science* (Vol. 7, p. 671). Frontiers Media S.A. <https://doi.org/10.3389/fmars.2020.00671>
- Barbieux, M., Uitz, J., Gentili, B., Pasquero De Fommervault, O., Mignot, A., Poteau, A., et al. (2019). Bio-optical characterization of subsurface chlorophyll maxima in the Mediterranean Sea from a Biogeochemical-Argo float database. *Biogeosciences*, 16(6), 1321–1342. <https://doi.org/10.5194/bg-16-1321-2019>
- Barone, B., Coenen, A. R., Beckett, S. J., McGillicuddy, D. J., Weitz, J. S., & Karl, D. M. (2019). The ecological and biogeochemical state of the north pacific subtropical gyre is linked to sea surface height. *Journal of Marine Research*, 77, 215–245. <https://doi.org/10.1357/002224019828474241>
- Beckmann, A., & Hense, I. (2007). Beneath the surface: Characteristics of oceanic ecosystems under weak mixing conditions - A theoretical investigation. *Progress in Oceanography*, 75(4), 771–796. <https://doi.org/10.1016/j.pocean.2007.09.002>
- Bellacicco, M., Cornec, M., Organelli, E., Brewin, R. J. W., Neukermans, G., Volpe, G. (2019). Global variability of optical backscattering by non-algal particles from a biogeochemical-argo data set. *Geophysical Research Letters*, 46(16), 9767–9776. <https://doi.org/10.1029/2019GL084078>
- Bittig, H. C., Steinhoff, T., Claustre, H., Fiedler, B., Williams, N. L., Sauzède, R., et al. (2018). An alternative to static climatologies: Robust estimation of open ocean CO₂ variables and nutrient concentrations from T, S, and O₂ data using Bayesian neural networks. *Frontiers in Marine Science*, 5, 328. <https://doi.org/10.3389/fmars.2018.00328>
- Brannigan, L. (2016). Intense submesoscale upwelling in anticyclonic eddies. *Geophysical Research Letters*, 43(7), 3360–3369. <https://doi.org/10.1002/2016GL067926>
- Brown, S. L., Landry, M. R., Selph, K. E., Jin Yang, E., Rii, Y. M., & Bidigare, R. R. (2008). Diatoms in the desert: Plankton community response to a mesoscale eddy in the subtropical North Pacific. *Deep-Sea Research Part II: Topical Studies in Oceanography*, 55(10–13), 1321–1333. <https://doi.org/10.1016/j.dsr2.2008.02.012>
- Cetinić, I., Perry, M. J., Briggs, N. T., Kallin, E., D'Asaro, E. A., & Lee, C. M. (2012). Particulate organic carbon and inherent optical properties during 2008 North Atlantic bloom experiment. *Journal of Geophysical Research*, 117(C6), C06028. <https://doi.org/10.1029/2011JC007771>
- Chai, F., Johnson, K. S., Claustre, H., Xing, X., Wang, Y., Boss, E., et al. (2020). Monitoring ocean biogeochemistry with autonomous platforms. *Nature Reviews Earth & Environment*, 1(6), 315–326. <https://doi.org/10.1038/s43017-020-0053-y>
- Chaigneau, A., Eldin, G., & Dewitte, B. (2009). Eddy activity in the four major upwelling systems from satellite altimetry (1992–2007). *Progress in Oceanography*, 83(1–4), 117–123. <https://doi.org/10.1016/j.pocean.2009.07.012>
- Chaigneau, A., Gizolme, A., & Grados, C. (2008). Mesoscale eddies off Peru in altimeter records: Identification algorithms and eddy spatio-temporal patterns. *Progress in Oceanography*, 79(2–4), 106–119. <https://doi.org/10.1016/j.pocean.2008.10.013>
- Chelton, D. B., Schlax, M. G., & Samelson, R. M. (2011). Global observations of nonlinear mesoscale eddies. *Progress in Oceanography*, 91(2), 167–216. <https://doi.org/10.1016/j.pocean.2011.01.002>
- Chelton, D. B., Schlax, M. G., Samelson, R. M., & de Szoeke, R. A. (2007). Global observations of large oceanic eddies. *Geophysical Research Letters*, 34(15), L15606. <https://doi.org/10.1029/2007GL030812>
- Claustre, H., Johnson, K. S., & Takeshita, Y. (2020). Observing the global ocean with biogeochemical-argo. *Annual Review of Marine Science*, 12, 23–48. <https://doi.org/10.1146/annurev-marine-010419-010956>
- Cornec, M., Claustre, H., Mignot, A., Guidi, L., Lacour, L., Poteau, A., et al. (2021). Deep chlorophyll maxima in the global ocean: Occurrences, drivers and characteristics. *Global Biogeochemical Cycles*, 35(4), e2020GB006759. <https://doi.org/10.1029/2020gb006759>
- Cullen, J. J. (2015). Subsurface chlorophyll maximum layers: Enduring enigma or mystery solved? *Annual Review of Marine Science*, 7(1), 207–239. <https://doi.org/10.1146/annurev-marine-010213-135111>
- de Boyer Montégut, C., Madec, G., Fischer, A. S., Lazar, A., & Iudicone, D. (2004). Mixed layer depth over the global ocean: An examination of profile data and a profile-based climatology. *Journal of Geophysical Research*, 109(C12), 1–20. <https://doi.org/10.1029/2004JC002378>
- Dufois, F., Hardman-Mountford, N. J., Greenwood, J., Richardson, A. J., Feng, M., Herbet, S., & Matear, R. (2014). Impact of eddies on surface chlorophyll in the South Indian Ocean. *Journal of Geophysical Research: Oceans*, 119(11), 8061–8077. <https://doi.org/10.1002/2014JC010164>
- Dufois, F., Hardman-Mountford, N. J., Greenwood, J., Richardson, A. J., Feng, M., & Matear, R. J. (2016). Anticyclonic eddies are more productive than cyclonic eddies in subtropical gyres because of winter mixing. *Science Advances*, 2(5), e1600282. <https://doi.org/10.1126/sciadv.1600282>
- Estrada, M., Marrasé, C., Latasa, M., Berdalet, E., Delgado, M., & Riera, T. (1993). Variability of deep chlorophyll maximum characteristics in the Northwestern Mediterranean. *Marine Ecology Progress Series*, 92(3), 289–300. <https://doi.org/10.2307/2483253410.3354/meps092289>
- Falkowski, P. G., Ziemann, D., Kolber, Z., & Bienfang, P. K. (1991). Role of eddy pumping in enhancing primary production in the ocean. *Nature*, 352(6330), 55–58. <https://doi.org/10.1038/352055a0>
- Fennel, K., & Boss, E. (2003). Subsurface maxima of phytoplankton and chlorophyll: Steady-state solutions from a simple model. *Limnology & Oceanography*, 48(4), 1521–1534. <https://doi.org/10.4319/lo.2003.48.4.1521>
- Frenger, I., Münnich, M., & Gruber, N. (2018). Imprint of Southern Ocean mesoscale eddies on chlorophyll. *Biogeosciences*, 15(15), 4781–4798. <https://doi.org/10.5194/bg-15-4781-2018>
- Gao, W., Wang, Z., & Zhang, K. (2017). Controlling effects of mesoscale eddies on thermohaline structure and in situ chlorophyll distribution in the western North Pacific. *Journal of Marine Systems*, 175, 24–35. <https://doi.org/10.1016/j.jmarsys.2017.07.002>
- Gaube, P., McGillicuddy, D. J., Chelton, D. B., Behrenfeld, M. J., & Strutton, P. G. (2014). Regional variations in the influence of mesoscale eddies on near-surface chlorophyll. *Journal of Geophysical Research: Oceans*, 119(12), 8195–8220. <https://doi.org/10.1002/2014JC010111>
- Gregg, W. W., & Carder, K. L. (1990). A simple spectral solar irradiance model for cloudless maritime atmospheres. *Limnology & Oceanography*, 35(8), 1657–1675. <https://doi.org/10.4319/lo.1990.35.8.1657>
- Guidi, L., Calil, P. H. R., Duhamel, S., Björkman, K. M., Doney, S. C., Jackson, G. A., et al. (2012). Does eddy-eddy interaction control surface phytoplankton distribution and carbon export in the North Pacific Subtropical Gyre? *Journal of Geophysical Research*, 117(2), G02024. <https://doi.org/10.1029/2012JG001984>

- Hanson, C. E., Pesant, S., Waite, A. M., & Pattiaratchi, C. B. (2007). Assessing the magnitude and significance of deep chlorophyll maxima of the coastal eastern Indian Ocean. *Deep-Sea Research Part II: Topical Studies in Oceanography*, 54(8–10), 884–901. <https://doi.org/10.1016/j.dsr2.2006.08.021>
- Herbland, A., & Voituriez, B. (1979). Hydrological structure analysis for estimating the primary production in the tropical Atlantic Ocean. *Journal of Marine Research*, 37(1), 87–101.
- Hopkinson, B. M., & Barbeau, K. A. (2008). Interactive influences of iron and light limitation on phytoplankton at subsurface chlorophyll maxima in the eastern North Pacific. *Limnology & Oceanography*, 53(4), 1303–1318. <https://doi.org/10.4319/lo.2008.53.4.1303>
- Huisman, J., Pham Thi, N. N., Karl, D. M., & Sommeijer, B. (2006). Reduced mixing generates oscillations and chaos in the oceanic deep chlorophyll maximum. *Nature*, 439(7074), 322–325. <https://doi.org/10.1038/nature04245>
- Joint, I., & Groom, S. B. (2000). Estimation of phytoplankton production from space: Current status and future potential of satellite remote sensing. *Journal of Experimental Marine Biology and Ecology*, 250(1–2), 233–255. [https://doi.org/10.1016/S0022-0981\(00\)00199-4](https://doi.org/10.1016/S0022-0981(00)00199-4)
- Jyothibabu, R., Vinayachandran, P. N., Madhu, N. V., Robin, R. S., Karnan, C., Jagadeesan, L., & Anjusha, A. (2015). Phytoplankton size structure in the southern Bay of Bengal modified by the Summer Monsoon Current and associated eddies: Implications on the vertical biogenic flux. *Journal of Marine Systems*, 143, 98–119. <https://doi.org/10.1016/j.jmarsys.2014.10.018>
- Klausmeier, C. A., & Litchman, E. (2001). Algal games: The vertical distribution of phytoplankton in poorly mixed water columns. *Limnology & Oceanography*, 46(8), 1998–2007. <https://doi.org/10.4319/lo.2001.46.8.1998>
- Klein, P., & Lapeyre, G. (2009). The oceanic vertical pump induced by mesoscale and submesoscale turbulence. *Annual Review of Marine Science*, 1(1), 351–375. <https://doi.org/10.1146/annurev.marine.010908.163704>
- Lacour, L., Ardyna, M., Stec, K. F., Claustre, H., Prieur, L., Poteau, A., et al. (2017). Unexpected winter phytoplankton blooms in the North Atlantic subpolar gyre. *Nature Geoscience*, 10(11), 836–839. <https://doi.org/10.1038/NGEO3035>
- Laxenaire, R., Speich, S., Blanke, B., Chaigneau, A., Pegliasco, C., & Stegner, A. (2018). Anticyclonic eddies connecting the western boundaries of Indian and Atlantic Oceans. *Journal of Geophysical Research: Oceans*, 123(11), 7651–7677. <https://doi.org/10.1029/2018JC014270>
- Laxenaire, R., Speich, S., & Stegner, A. (2019). Evolution of the thermohaline structure of one Agulhas ring reconstructed from satellite altimetry and Argo floats. *Journal of Geophysical Research: Oceans*, 124(12), 8969–9003. <https://doi.org/10.1029/2018JC014426>
- Laxenaire, R., Speich, S., & Stegner, A. (2020). Agulhas ring heat content and transport in the South Atlantic estimated by combining satellite altimetry and Argo profiling floats data. *Journal of Geophysical Research: Oceans*, 125(9), e2019JC015511. <https://doi.org/10.1029/2019JC015511>
- Letelier, R. M., Karl, D. M., Abbott, M. R., & Bidigare, R. R. (2004). Light driven seasonal patterns of chlorophyll and nitrate in the lower euphotic zone of the North Pacific Subtropical Gyre. *Limnology & Oceanography*, 49(2), 508–519. <https://doi.org/10.4319/lo.2004.49.2.0508>
- Letelier, R. M., Karl, D. M., Abbott, M. R., Flament, P., Freilich, M., Lukas, R., & Strub, T. (2000). Role of late winter mesoscale events in the biogeochemical variability of the upper water column of the North Pacific Subtropical Gyre. *Journal of Geophysical Research*, 105(C12), 28723–28739. <https://doi.org/10.1029/1999jc000306>
- Lévy, M., Klein, P., & Treguier, A. M. (2001). Impact of sub-mesoscale physics on production and subduction of phytoplankton in an oligotrophic regime. *Journal of Marine Research*, 59(4), 535–565. <https://doi.org/10.1357/002224001762842181>
- Li, Q. P., & Hansell, D. A. (2016). Mechanisms controlling vertical variability of subsurface chlorophyll maxima in a mode-water eddy. *Journal of Marine Research*, 74, pp. 175–199. <https://doi.org/10.1357/002224016819594827>
- Loisel, H., & Morel, A. (1998). Light scattering and chlorophyll concentration in case 1 waters: A reexamination. *Limnology & Oceanography*, 43(5), 847–858. <https://doi.org/10.4319/lo.1998.43.5.0847>
- Mahadevan, A. (2016). The impact of submesoscale physics on primary productivity of Plankton. *Annual Review of Marine Science*, 8(1), 161–184. <https://doi.org/10.1146/annurev-marine-010814-015912>
- Mahadevan, A., D'Asaro, E., Lee, C., & Perry, M. J. (2012). Eddy-driven stratification initiates North Atlantic spring phytoplankton blooms. *Science*, 336(6090), 54–58. <https://doi.org/10.1126/science.1218740>
- Martin, J., Tremblay, J. É., Gagnon, J., Tremblay, G., Lapoussière, A., Jose, C., et al. (2010). Prevalence, structure and properties of subsurface chlorophyll maxima in Canadian Arctic waters. *Marine Ecology Progress Series*, 412, 69–84. <https://doi.org/10.3354/meps08666>
- McGillicuddy, D. J. (2016). Mechanisms of physical-biological-biochemical interaction at the oceanic mesoscale. In *Annual Review of Marine Science*. 8(1), 125–159. <https://doi.org/10.1146/annurev-marine-010814-015606>
- McGillicuddy, D. J., Anderson, L. A., Bates, N. R., Bibby, T., Buesseler, K. O., Carlson, C. A., et al. (2007). Eddy/Wind interactions stimulate extraordinary mid-ocean plankton blooms. *Science*, 316(5827), 1021–1026. <https://doi.org/10.1126/science.1136256>
- McGillicuddy, D. J., Robinson, A. R., Siegel, D. A., Jannasch, H. W., Johnson, R., Dickey, T. D., et al. (1998). Influence of mesoscale eddies on new production in the Sargasso Sea. *Nature*, 394(6690), 263–266. <https://doi.org/10.1038/28367>
- Mignot, A., Claustre, H., Uitz, J., Poteau, A., D'Ortenzio, F., & Xing, X. (2014). Understanding the seasonal dynamics of phytoplankton biomass and the deep chlorophyll maximum in oligotrophic environments: A Bio-Argo float investigation. *Global Biogeochemical Cycles*, 28(8), 856–876. <https://doi.org/10.1002/2013GB004781>
- Morel, A., Huot, Y., Gentili, B., Werdell, P. J., Hooker, S. B., & Franz, B. A. (2007). Examining the consistency of products derived from various ocean color sensors in open ocean (Case 1) waters in the perspective of a multi-sensor approach. *Remote Sensing of Environment*, 111(1), 69–88. <https://doi.org/10.1016/j.rse.2007.03.012>
- Pasquero De Fommervault, O., Perez-Brunius, P., Damien, P., Camacho-Ibar, V. F., & Sheinbaum, J. (2017). Temporal variability of chlorophyll distribution in the Gulf of Mexico: Bio-optical data from profiling floats. *Biogeosciences*, 14(24), 5647–5662. <https://doi.org/10.5194/bg-14-5647-2017>
- Platt, T., Sathyendranath, S., Caverhill, C. M., & Lewis, M. R. (1988). Ocean primary production and available light: Further algorithms for remote sensing. *Deep-Sea Research Part A. Oceanographic Research Papers*, 35(6), 855–879. [https://doi.org/10.1016/0198-0149\(88\)90064-7](https://doi.org/10.1016/0198-0149(88)90064-7)
- Roemmich, D., Alford, M. H., Claustre, H., Johnson, K. S., King, B., Moum, J., et al. (2019). On the future of Argo: A global, full-depth, multi-disciplinary array. *Frontiers in Marine Science*, 6, 439. <https://doi.org/10.3389/fmars.2019.00439>
- Roesler, C., Uitz, J., Claustre, H., Boss, E., Xing, X., Organelli, E., et al. (2017). Recommendations for obtaining unbiased chlorophyll estimates from in situ chlorophyll fluorometers: A global analysis of WET Labs ECO sensors. *Limnology and Oceanography: Methods*, 15(6), 572–585. <https://doi.org/10.1002/lom3.10185>
- Sauzède, R., Bittig, H. C., Claustre, H., de Fommervault, O. P., Gattuso, J. P., Legendre, L., & Johnson, K. S. (2017). Estimates of water-column nutrient concentrations and carbonate system parameters in the global ocean: A novel approach based on neural networks. *Frontiers in Marine Science*, 4, 128. <https://doi.org/10.3389/fmars.2017.00128>
- Siegel, D. A., Behrenfeld, M. J., Maritorea, S., McClain, C. R., Antoine, D., Bailey, S. W., et al. (2013). Regional to global assessments of phytoplankton dynamics from the SeaWiFS mission. *Remote Sensing of Environment*, 135, 77–91. <https://doi.org/10.1016/j.rse.2013.03.025>

- Siegel, D. A., Court, D. B., Menzies, D. W., Peterson, P., Maritorena, S., & Nelson, N. B. (2008). Satellite and in situ observations of the bio-optical signatures of two mesoscale eddies in the Sargasso Sea. *Deep-Sea Research Part II: Topical Studies in Oceanography*, 55(10–13), 1218–1230. <https://doi.org/10.1016/j.dsr2.2008.01.012>
- Siegel, D. A., Peterson, P., McGillicuddy, D. J., Maritorena, S., & Nelson, N. B. (2011). Bio-optical footprints created by mesoscale eddies in the Sargasso Sea. *Geophysical Research Letters*, 38(13), L13608. <https://doi.org/10.1029/2011GL047660>
- Silsbe, G. M., & Malkin, S. Y. (2016). Where light and nutrients collide: The global distribution and activity of subsurface chlorophyll maximum layers. In *Aquatic microbial ecology and biogeochemistry: A dual perspective* (pp. 1–152). https://doi.org/10.1007/978-3-319-30259-1_12
- Steele, J. H. (1964). A study of the production in the Gulf of Mexico. *Journal of Marine Research*, 22, 211–222.
- Stramski, D., Reynolds, R. A., Kahru, M., & Mitchell, B. G. (1999). Estimation of particulate organic carbon in the ocean from satellite remote sensing. *Science*, 285, 239–242. <https://doi.org/10.1126/science.285.5425.239>
- Sweeney, E. N., McGillicuddy, D. J., & Buesseler, K. O. (2003). Biogeochemical impacts due to mesoscale eddy activity in the Sargasso Sea as measured at the Bermuda Atlantic Time-series Study (BATS). *Deep-Sea Research Part II: Topical Studies in Oceanography*, 50(22–26), 3017–3039. <https://doi.org/10.1016/j.dsr2.2003.07.008>
- Uz, B. M., Yoder, J. A., & Osychny, V. (2001). Pumping of nutrients to ocean surface waters by the action of propagating planetary waves. *Nature*, 409(6820), 597–600. <https://doi.org/10.1038/35054527>
- Vaillancourt, R. D., Marra, J., Seki, M. P., Parsons, M. L., & Bidigare, R. R. (2003). Impact of a cyclonic eddy on phytoplankton community structure and photosynthetic competency in the subtropical North Pacific Ocean. *Deep-Sea Research Part I: Oceanographic Research Papers*, 50, 829–847. [https://doi.org/10.1016/S0967-0637\(03\)00059-1](https://doi.org/10.1016/S0967-0637(03)00059-1)
- Waga, H., Hirawake, T., & Ueno, H. (2019). Impacts of mesoscale eddies on phytoplankton size structure. *Geophysical Research Letters*, 46(22), 13191–13198. <https://doi.org/10.1029/2019GL085150>
- Waite, A. M., Muhling, B. A., Holl, C. M., Beckley, L. E., Montoya, J. P., Strzelecki, J., et al. (2007). Food web structure in two counter-rotating eddies based on $\delta^{15}\text{N}$ and $\delta^{13}\text{C}$ isotopic analyses. *Deep-Sea Research Part II: Topical Studies in Oceanography*, 54(8–10), 1055–1075. <https://doi.org/10.1016/j.dsr2.2006.12.010>
- Wong, A., Keeley, R., Carval, T., & the Argo Data Management Team (2020). *Argo quality control manual technical report*. ArgoData Management team.
- Xiu, P., & Chai, F. (2020). Eddies affect subsurface phytoplankton and oxygen distributions in the North Pacific Subtropical Gyre. *Geophysical Research Letters*, 47(15), e2020GL087037. <https://doi.org/10.1029/2020GL087037>